Envelope burning over-luminosity:
a challenge to synthetic TP-AGB models

P. Marigo[1,2]

[1] Max-Planck-Institut für Astrophysik, Karl-Schwarzschild-Strasse 1, D-87540 Garching bei München, Germany
[2] Department of Astronomy, University of Padova, Vicolo dell'Osservatorio 5, I-35122 Padova, Italy

Abstract. Until recently synthetic AGB models had not taken into account the break-down of the core mass-luminosity ($M_c - L$) relation due to the occurrence of envelope burning in the most massive ($M \gtrsim 3.5\,M_\odot$ for Pop. II and $M \gtrsim 4.5\,M_\odot$ for Pop. I) and luminous ($M_{\rm bol} \lesssim -6$) stars.

Marigo et al. (1998) made the first attempt to consistently include the related over-luminosity effect (i.e. above the $M_c - L$ relation) in synthetic TP-AGB calculations. The method couples complete envelope integrations with analytical prescriptions, these latter being presently updated with the highly detailed relations by Wagenhuber & Groenewegen (1998).

In this paper the reliability of the solution scheme is tested by comparison with the results of complete evolutionary calculations for a $7\,M_\odot$ AGB star undergoing envelope burning (Blöcker & Schönberner 1991; Blöcker 1995).

Indeed, the method proves to be valid as it is able to reproduce with remarkable accuracy several evolutionary features of the $7\,M_\odot$ star (e.g. rate of brightening, luminosity evolution as a function of the core mass and envelope mass for different mass-loss prescriptions) as predicted by full AGB models.

Basing on the new solution method, we present extensive synthetic TP-AGB calculations for stars with initial masses of 3.5, 4.0, 4.5, and $5.0\,M_\odot$, and three choices of the initial metallicity, i.e. $Z = 0.019$, $Z = 0.008$, and $Z = 0.004$. Three values of the mixing-length parameter are used, i.e. $\alpha = 1.68$, 2.0, 2.5.

We investigate the dependence of envelope burning on such stellar parameters (M, Z, and α). The comparison between different cases gives hints on the interplay between envelope burning over-luminosity and mass loss, and related effects on TP-AGB lifetimes.

Key words: stars: mass-loss – stars: AGB and post-AGB – stars: evolution

1. Introduction

Synthetic AGB models may provide a powerful tool of investigation (Renzini & Voli 1981; Groenewegen & de Jong 1993; Marigo et al. 1996a). Evolutionary calculations can be easily

carried out over the whole mass range of AGB stars and for various metallicities, and the results tested according to the adoption of various input prescriptions (e.g. analytical relations derived from full AGB models, mass-loss laws, parameters of the third dredge-up). In this way, it is possible to explore the sensitiveness of theoretical predictions to different physical assumptions and, at the same time, to readily get an overall picture of aspects related both to single star evolution (e.g. location on the H-R diagram, maximum AGB luminosities, stellar lifetimes, initial mass-final mass relation, changes in the surface chemical composition, stellar yields) and to integrated properties of the stellar aggregates in which AGB stars are present (e.g. luminosity functions of oxygen- and carbon-rich AGB stars, contribution of evolved stars to the integrated light and to the chemical enrichment of the host galaxy).

Of course, the computational agility and flexibility typical of the synthetic approach are paid with a certain loss of details if compared to complete AGB models. However, in order to get reliable results from synthetic analyses the degree of approximation in treating the physical processes must be good enough so that no essential feature is missed.

Actually, a clear point of inadequacy of synthetic AGB models has so far concerned the treatment of envelope burning in the most massive stars ($M \gtrsim 3.5\,M_\odot$). In brief, the erroneous assumption common to AGB analyses performed either with the aid of convective envelope models (Scalo et al. 1975; Renzini & Voli 1981; Marigo et al. 1996a), or purely analytical prescriptions (Groenewegen & de Jong 1993) is that the quiescent surface luminosity of a TP-AGB star experiencing envelope burning still obeys the standard $M_c - L$ relation, as in the case of lower mass stars ($M \lesssim 3.5\,M_\odot$).

On the contrary, over the years complete AGB calculations have clearly indicated that nuclear burning in the hottest convective envelope layers of the most massive TP-AGB stars may be a considerable energy source, making these stars depart significantly from the $M_c - L$ relation towards higher luminosities (Blöcker & Schönberner 1991 (hereinafter also BS91); Lattanzio 1992; Boothroyd & Sackmann 1992; Vassiliadis & Wood 1993; Blöcker 1995 (hereinafter also B95); Wagenhuber 1996).

Indeed, the recent discovery of the over-luminosity produced by envelope burning above the $M_c - L$ relation has no-

tably changed and improved our current understanding of the AGB phase, setting important implications.

In principle, the luminosity increase of a TP-AGB star is not bounded by the classical AGB luminosity limit of $M_{bol} \sim -7.1$, predicted by the Paczyński (1970) $M_c - L$ relation for a mass of the degenerate core equal to the Chandrasekhar critical value of $\sim 1.4\,M_\odot$ (BS91). For this reason, the observation of AGB stars with luminosities close to $M_{bol} \sim -7.1$ does not imply that their core masses are close to $1.4\,M_\odot$, a circumstance that has been until recently considered as a supporting indirect evidence for the occurrence of Type $I_{1/2}$ Supernovae, due to disruptive carbon ignition (see, for instance, Wood et al. 1983).

Moreover, the maximum quiescent luminosity, L_{max}, attained by an AGB star with envelope burning does not coincide with the final luminosity at the so-called AGB tip, as in the case of lower mass stars following the core mass-luminosity relation. In higher mass stars the maximum of the luminosity occurs, in practice, at the onset of the superwind, and hence before the AGB tip is reached (when the envelope has been almost completely ejected and the core mass-luminosity relation is recovered).

It follows that at high luminosities, say $M_{bol} < -6.5$, the core-mass luminosity relation cannot be longer employed in combination with the initial mass-final mass $(M_i - M_f)$ relation to estimate the age of a coeval system on the base of its brightest AGB stars (usually inferred through the steps: $L_{max} \rightarrow M_f \rightarrow M_i \rightarrow$ age; see for instance the review by Iben & Renzini (1983)).

The over-luminosity effect is also expected to intensify the mass-loss process suffered by stars with envelope burning, so as to possibly anticipate the onset of the superwind regime. Then, this would result in a reduction of the TP-AGB lifetimes and hence of the remnant white dwarf masses. Then, in the case envelope burning takes place already in stars with relatively low core masses (i.e. $M_c \gtrsim 0.7$–$0.8\,M_\odot$), the latter consequence may concur to solve the long-standing problem related to the excess of white dwarfs more massive than $\sim 0.7\,M_\odot$, as predicted by synthetic AGB models (see Bragaglia et al. (1995) for a discussion of this point).

In this context, Marigo et al. (1998) first pointed out a possible solution scheme to overcome the limit of synthetic models. This paper aims at verifying the validity of the original treatment of envelope burning – coupling the use of analytical relationships with complete envelope integrations – by testing its capability of reproducing the results from full AGB calculations.

The general organisation of the paper is as follows. In Sect. 2 the rationale underlying envelope integrations is briefly recalled, together with the main analytical prescriptions. In Sect. 3 the validity of the method is checked by comparison with full evolutionary calculations for a $7\,M_\odot$ star performed by BS91 and B95. Sect. 4 presents the results of synthetic TP-AGB evolutionary calculations for stars with initial masses in the range $3.5\,M_\odot \leq M \leq 5.0\,M_\odot$, and initial metallicities $Z = 0.019$, $Z = 0.008$, and $Z = 0.004$. The sensitiveness of envelope burning to stellar mass, metallicity, and mixing-length parameter is discussed in Sect. 5. Some relevant quantities char-

acterising the evolution of the model stars are tabulated in Table 2. Finally, Sect. 6 contains some concluding remarks and illustrates the intents of future works.

2. Outline of the method

The reader is referred to the work by Marigo et al. (1998) for a detailed description of the method developed to calculate the energy contribution from envelope burning to the stellar luminosity. Let us herein just summarise the basic points.

Given the total stellar mass M, the core mass M_c, and the chemical composition of the convective envelope at each time during the quiescent inter-flash periods, the surface luminosity L is singled out by means of envelope integrations, provided that proper boundary conditions are fulfilled.

In this way, the erroneous assumption $L = L_{M_c}$ – where L_{M_c} corresponds to the luminosity predicted by the $M_c - L$ relation for a given core mass – is abandoned. Moreover, the usual prescription, fixing $L_r = constant = L_{M_c}$ throughout the envelope, is replaced with the equation of energy balance under *static approximation* (i.e. the entropy term $-T \partial S / \partial t$ is neglected):

$$\frac{\partial L_r}{\partial M_r} = \epsilon_r \tag{1}$$

so that the complete set of the stellar structure equations must be integrated.

In general, the determination of the unknown functions r, P_r, T_r, L_r across the envelope requires to specify four boundary conditions. For any given pair of envelope parameters, L and T_{eff}, two conditions naturally derive from the integration of the photospheric equations for T and P down to the bottom of the photosphere (Kippenhahn et al. 1967). Then, since both L and T_{eff} are actually free parameters in our static envelope model, two more boundary conditions must be fixed.

In pursuit of this aim, we express the quiescent surface luminosity L as:

$$L = L_G + L_{He} - L_\nu + L_H + L_{EB} \tag{2}$$

where L_G represents the rate of energy generation due to the gravitational contraction of the core; L_{He} is the small energy contribution from the He-burning shell; L_ν is the rate of energy loss via neutrinos; L_H and L_{EB} refer to the rate of energy production by hydrogen burning in *radiative* and *convective* conditions, respectively.

We remark that the gravitational contribution is included only in the energetic budget via the term L_G, but according to the *static approximation* used in our model, we do not actually take into account the possible contraction and/or expansion of the structure during the evolution.

It is worth noticing that the energy contributions indicated in the right hand-side of Eq. (2) are produced within distinct regions of the star. Specifically, $(L_G + L_{He} - L_\nu)$ represents the net rate of energy outflow from the core, this latter being commonly defined as the stellar interior below the H-He discontinuity. Beyond the core, energy is produced by nuclear burning

of hydrogen, at a total rate given by the the sum of the two terms ($L_H + L_{EB}$). It results that $L_{EB} = 0$ in low-mass TP-AGB stars ($M \lesssim 3.5\,M_\odot$) complying with the $M_c - L$ relation (i.e. without envelope burning). Differently, the term L_{EB} can significantly contribute to the energy budget of more massive TP-AGB stars ($M > 3.5\,M_\odot$), as the base of the convective envelope penetrates into the H-burning shell.

In virtue of the site separation of the energy sources, it is convenient to set the two boundary conditions in question by specifying the local values of the luminosity L_r at two suitable transition points, provided that Eq. (2) is satisfied. Denoting by R_{core} and R_{conv} the radial coordinates of the bottom of the H-burning shell (i.e. where hydrogen abundance is zero, below which the mass M_c is contained) and the base of the convective envelope, respectively, we can write:

$$L(r = R_{core}) = L_G + L_{He} - L_\nu \tag{3}$$
$$L(r = R_{conv}) = L(r = R_{core}) + L_H \tag{4}$$

with the right hand-side members of both equations being known functions of the core mass, envelope mass, and chemical composition (see Sect. 2.1 for the adopted prescriptions).

Then, Eqs. (3) and (4) together with the photospheric conditions provide the four boundary constraints necessary to determine the entire envelope structure. Numerical integrations of the envelope are performed with a very fine mass resolution, the width of the innermost shells (where the structural gradients become extremely steep) typically amounting to 10^{-7}–$10^{-8}\,M_\odot$.

The solution model yields, in particular, the quantity L_{EB}, i.e. the energy produced within the convective envelope, and the (L, T_{eff}) pair, i.e. the current location on the H-R diagram, without invoking further external assumptions.

2.1. Prescriptions for ($L_G + L_{He} - L_\nu$) and L_H

The boundary conditions expressed by Eqs. (3) and (4) imply the knowledge of the luminosity contributions:

- ($L_G + L_{He} - L_\nu$) from the core
- L_H from radiative hydrogen burning

To this aim, we adopt the analytical formulae describing the light curves of TP-AGB stars, presented by Wagenhuber & Groenewegen (1998, hereafter also WG98). These prescriptions are a high accuracy reproduction of the results from extensive grids of complete evolutionary calculations carried out by Wagenhuber (1996) for stars with initial masses in the range $0.8\,M_\odot \leq M \leq 7.0\,M_\odot$, and metallicities $Z = 0.0001$, $Z = 0.008$, and $Z = 0.02$.

The maximum luminosity during quiescent H-burning is expressed as the sum of different terms:

$$L = (18160 + 3980 \log \tfrac{Z}{0.02})(M_c - 0.4468) \tag{5a}$$
$$+10^{2.705 + 1.649\,M_c} \tag{5b}$$
$$\times 10^{0.0237(\alpha - 1.447)\,M_{c,0}^2\,M_{env}^2(1 - e^{-\Delta M_c/0.01})} \tag{5c}$$
$$-10^{3.529 - (M_{c,0} - 0.4468)\Delta M_c/0.01} \tag{5d}$$

where Z denotes the metallicity, $M_{c,0}$ is the core mass at the first thermal pulse (see Table 2), $\Delta M_c = M_c - M_{c,0}$ gives the actual increment of the core mass, and M_{env} is the current envelope mass. Masses and luminosities are expressed in solar units.

The first term (5a) represents the usual linear $M_c - L$ relation, giving the quiescent luminosity of TP-AGB stars already in the full amplitude regime, with core masses in the range $0.6\,M_\odot \lesssim M_c \lesssim 0.95\,M_\odot$. The second term (5b) provides a correction becoming significant for high values of the core mass, $M_c > 0.95\,M_\odot$. The third term (5c) accounts for the over-luminosity produced by envelope burning (i.e. the L_{EB} term of Eq. (2)), as a function of the envelope mass M_{env}. A dependence on the mixing-length parameter, α, is included to reproduce the results from full calculations (i.e. Wagenhuber (1996) with $\alpha = 1.5$, Blöcker (1995) with $\alpha = 2$, D'Antona & Mazzitelli (1996) with $\alpha = 2.75$). Finally, the fourth term (5d) gives a negative correction to the luminosity in order to mimic the sub-luminous and steep evolution typical of the first pulses.

The nice distinction between various terms in Eq. (5) allows us to derive the term $L - L_{EB}$, that is the contribution of all energy sources but for envelope burning. This is an important point indeed, since L_{EB} is just the quantity we aim at evaluating by means of envelope integrations as described in Sect. 2. The luminosity produced by envelope burning can be eliminated from Eq. (5), by setting the corresponding term (5c) equal to unity. For the sake of clarity in notation, let us denote by L_{M_c} the resulting luminosity:

$$L_{M_c} = (18160 + 3980 \log \tfrac{Z}{0.02})(M_c - 0.4468) \tag{6a}$$
$$+10^{2.705 + 1.649 M_c} \tag{6b}$$
$$-10^{3.529 - (M_{c,0} - 0.4468)\Delta M_c/0.01} \tag{6c}$$

Hereinafter, we will refer to Eq. (6) as the standard $M_c - L$ relation adopted in this study.

This relation replaces the formulae by Boothroyd & Sackmann (1988a) and Iben & Truran (1978), for different ranges of the core mass, used in previous works (Marigo et al. 1996ab,1998). The notable improvement is that the new prescription is based on homogeneous evolutionary calculations for a large range of core masses and metallicities. Moreover, it is worth remarking that the quantity $L - L_{EB}$ cannot be obtained when using the Iben & Truran's formula (1978), which is likely to mask a non-quantifiable contribution from a weak envelope burning (see Sect. 4.1 in Marigo et al. (1998)).

From the above scheme it follows that the energy contribution from envelope burning, L_{EB}, is supposed to satisfy the relation:

$$L = L_{M_c} + L_{EB} \tag{7}$$

In other words, we assume that the nuclear burning at the base of the convective envelope produces the excess of luminosity above the underlying $M_c - L$ relation.

According to Wagenhuber (1996) it is possible to derive L_H from:

$$\log\left(\frac{L_H}{L}\right) = -0.012 - 10^{-1.25 - 113\Delta M_c} - 0.0016\,M_{env} \tag{8}$$

where the variables are expressed in solar units. Since the above relation is an analytical fit to full calculations with no (or quite weak) envelope burning (i.e. $L_{EB} \sim 0$), we can safely assume $L = L_{M_c}$ in Eq. (8).

Hence, we can write:

$$L_H = f_H L_{M_c} \qquad (9)$$

where f_H is the fractional contribution of radiative H-burning to L_{M_c}, and

$$L_G + L_{He} - L_\nu = (1 - f_H) L_{M_c} \qquad (10)$$

is the complementary term to L_{M_c}, including the gravitational shrinking of the core, L_G, the shell He-burning, L_{He}, and neutrino losses, L_ν.

It turns out that, once the full amplitude regime has been established, these fractional luminosities attain typical values, slightly dependent on the core mass, envelope mass, and metallicity, of $L_H/L_{M_c} \sim 0.96 \div 0.98$ and $(L_G + L_{He} - L_\nu)/L_{M_c} \sim 0.04 \div 0.02$.

Finally, it is worth recalling the general validity of the method, which can be applied as well to solve the envelope structure of low-mass stars without envelope burning (i.e. $L_{EB} = 0$ and $L = L_{M_c}$).

2.2. Other analytical prescriptions

The general structure of the synthetic TP-AGB model is the same as described in Marigo et al. (1996a, 1998). With respect to these latter works, some input prescriptions have been updated thanks to the recent re-determinations by Wagenhuber (1996) and WG98. Besides the $M_c - L$ relation already quoted in Sect. 2.1, the other new analytical prescriptions are:

– The core mass - interpulse period relation:

$$\log t_{ip} = (-3.628 + 0.1337 \ \log \frac{Z}{0.02}) \ (M_c - 1.9454) \qquad (10a)$$
$$-10^{-2.080 - 0.353 \ \log \frac{Z}{0.02} + 0.200(M_{env} + \alpha - 1.5)} \qquad (10b)$$
$$-10^{-0.626 - 70.30 \ (M_{c,0} - \log \frac{Z}{0.02}) \ \Delta M_c} \qquad (10c)$$

Here three components can be distinguished, namely: the term (10a) expresses the interpulse period t_{ip} (in yr) as a decreasing exponential function of M_c with some dependence on the metallicity; the term (10b) gives a negative correction to include the effect of envelope burning in somewhat reducing the inter-pulse period; and term (10c) reproduces the initial increase of t_{ip} starting from values that are shorter by almost a factor of two compared to those derived from the asymptotic relation for the same core mass.

– The rate of evolution of the hydrogen-exhausted core:

$$\frac{dM_c}{dt} = q \frac{L_H}{X} \qquad (M_\odot \ yr^{-1}) \qquad (11)$$

where

$$q = (1.02 + 0.017 \log \frac{Z}{0.02}) \ 10^{-11} \qquad (M_\odot \ L_\odot^{-1} \ yr^{-1}) \qquad (12)$$

with X and Z corresponding to the hydrogen and metal abundances (mass fractions) in the envelope, respectively.

3. Comparison with full calculations

The most meaningful test to check the reliability of the method developed to account envelope burning is to compare the predictions of the synthetic TP-AGB models with those from complete AGB evolutionary calculations. We consider the results obtained by BS91 and B95 for a TP-AGB star with initial mass of $7 \, M_\odot$ and chemical composition $[X = 0.739, Y = 0.240, Z = 0.021]$.

We calculate the synthetic TP-AGB evolution of the $7 \, M_\odot$ star starting from the same initial conditions at the first thermal pulse as in BS91, i.e. with $M = 6.871 \, M_\odot, M_c = 0.91335 \, M_\odot, L = 25217 L_\odot$. Specifically, the underlying $M_c - L$ relation is that given by WG98 (Eq. (6)), multiplied by a proper factor of 1.16. This latter is calibrated in order to obtain the same value of the luminosity at the first thermal pulse as in BS91.

In our envelope model the mixing-length parameter is set equal to $\alpha = 2.3$ so as to obtain values of the effective temperature similar to those derived from full calculations (see Fig. 5 in B95), which were actually carried out with a lower value, $\alpha = 2.0$. This is most likely due to the different opacities employed in Blöcker's calculations (Cox & Stewart 1970), and in the present study (Iglesias & Rogers 1996; Alexander & Ferguson 1994).

As far as mass loss by stellar winds on the AGB is concerned, two are the prescriptions here adopted as in B95, so that we distinguish two cases:

1. the *BH case* referring to the use of the Baud & Habing's (1983) modification of Reimers' formula;
2. the *BH4 case* corresponding to the use of the Baud & Habing's law (1983) from the beginning of the AGB till a certain stage (i.e. when $M_c = 0.93537 \, M_\odot$ at the 26th pulse), beyond which a constant rate of $4 \times 10^{-4} \, M_\odot \ yr^{-1}$ is artificially introduced to mimic the onset of the superwind regime.

For more details the reader should refer to B95.

Figs. 1 (for the *BH case*) and 2 (for the *BH4 case*) show that the results of full calculations are remarkably well reproduced by our synthetic calculations. The displayed luminosity evolution refers to the pre-flash maximum values before the occurrence of each thermal pulse. The $7 \, M_\odot$ star starts to depart from the $M_c - L$ as soon as it enters the TP-AGB phase, quickly increasing its luminosity because of the occurrence of envelope burning.

In the *BH case* the luminosity is still steeply increasing when calculations have been interrupted (at the 30th pulse in BS91; at the 60th pulse in this work), due to the fact that the stellar mass has not yet been significantly reduced by stellar winds. Differently, the artificial onset of a superwind mass-loss rate in the *BH4 case* causes the quick ejection of the envelope over the subsequent $4 - 5$ interpulse periods. Our synthetic calculations quite well reproduce the overall features of the luminosity evolution, comprising the initial rising, the luminosity peak, the decline following the activation of the high mass-loss rate, and the final re-approaching towards the $M_c - L$ relation.

Table 1. A solar-metallicity 7 $M_\odot$ star with envelope burning: comparison between full TP-AGB modelling performed by Blöcker & Schönberner (1991) (BS91; *BH case*) and our calculations (M98), for four selected values of the core mass.

| BS91/M98	$N_{\rm P}$	$\frac{M_{\rm c}}{M_\odot}$	$\frac{M}{M_\odot}$	$\frac{\dot{M}}{M_\odot\,{\rm yr}}$	$\frac{L}{L_\odot}$	$|\epsilon_L|$	$\frac{L_{\rm EB}}{L_{\rm H}+L_{\rm EB}}$	$\frac{\dot{M}_{\rm bol}}{{\rm mag\,yr}}$
BS91	1	0.91335	6.871	$4.9\,10^{-7}$	25217		0.02	$-3.3\,10^{-5}$
M98	1	0.91335	6.871	$6.8\,10^{-7}$	25217	0.000	0.01	$-5.5\,10^{-5}$
BS91	10	0.92061	6.854	$1.1\,10^{-6}$	40268		0.30	$-1.4\,10^{-5}$
M98	11	0.92061	6.850	$1.1\,10^{-6}$	37788	0.062	0.33	$-1.5\,10^{-5}$
BS91	20	0.92970	6.821	$1.7\,10^{-6}$	51662		0.46	$-7.2\,10^{-6}$
M98	22	0.92970	6.807	$1.9\,10^{-6}$	51537	0.003	0.46	$-7.6\,10^{-6}$
BS91	30	0.93909	6.774	$2.1\,10^{-6}$	58806		0.52	$-4.0\,10^{-6}$
M98	34	0.93909	6.745	$2.6\,10^{-6}$	60760	0.033	0.51	$-3.4\,10^{-6}$

- $N_{\rm P}$: number of the pulse cycle
- $M_{\rm c}$: hydrogen-exhausted core
- M: current stellar mass
- $\dot{M}$: mass-loss rate
- L: quiescent surface luminosity
- $|\epsilon_L| = |\frac{L_{\rm M98}-L_{\rm BS91}}{L_{\rm BS91}}|$: percentage difference in the evaluation of L (at given $M_{\rm c}$) derived in the present work with respect to full calculations
- $\frac{L_{\rm EB}}{L_{\rm H}+L_{\rm EB}}$: fraction of the total hydrogen luminosity provided by envelope burning
- $\dot{M}_{\rm bol}$: rate of brightening

For purpose of comparison, the predicted TP-AGB evolution of a solar-metallicity 2.5 $M_\odot$ star is also plotted. No evidence of departure from the standard $M_{\rm c}-L$ relation shows up in this case. We point out that the relatively large number of thermal pulses (~ 25) suffered by the 2.5 $M_\odot$ model before reaching the $M_{\rm c}-L$ relation is due to the early onset of the third dredge-up (according to the scheme outlined in Sect. 4.1). In fact, the reduction of the core mass, which occurs every time a dredge-up event takes place, somewhat delays the onset of the full amplitude regime.

As far as the 7 $M_\odot$ star is concerned, different properties can be then compared, namely: i) the surface luminosity for given core mass and envelope mass; ii) the rate of brightening $\dot{M}_{\rm bol}$; iii) the fraction of the hydrogen luminosity produced at the hot base of the convective envelope $L_{\rm EB}/(L_{\rm H}+L_{\rm EB})$; iv) the current total mass; and v) the mass-loss rate. These quantities are indicated in Table 1 at fixed values of the core mass for four selected thermal pulses (*BH case*; in analogy with Table 1 of BS1).

The agreement is indeed satisfactory. The relative errors, $|\epsilon_L| = |L_{\rm M98} - L_{\rm BS91}|/L_{\rm BS91}$, of the surface luminosity estimated with our model, $L_{\rm M98}$, with respect to that obtained in the reference work, $L_{\rm BS91}$, do not exceed few percents in all cases. The very nice accordance can be better appreciated from Fig. 3, showing ϵ_L (solid line) as a function of the core mass for the entire sequence of thermal pulses calculated by BS91 for the *BH case* (top panel), and B95 for the *BH4 case* (bottom panel).

The values of ϵ_L are always quite small, also in consideration that the models are intrinsically different just because of the use of different input physics (e.g. opacities). Moreover, it is worth noticing that in the *BH case* the greatest differences in luminosity for given core mass occur just in correspondence
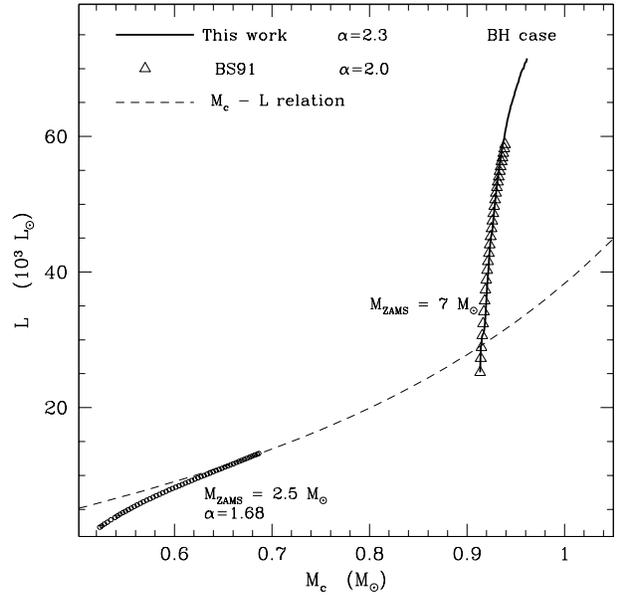
Fig. 1. Evolution of the surface luminosity as a function of the core mass for a 7 $M_\odot$ star with initial solar metallicity (i.e. $Z = 0.021$). The empty triangles refer to complete evolutionary calculations carried out by Blöcker & Schönberner (1991) from the 1st up to the 30th thermal pulse. The adopted mass-loss prescription is that suggested by Baud & Habing (1983; *BH case*). For comparison, the luminosity evolution predicted by our synthetic TP-AGB model is shown (solid line). Calculations are carried out starting from the same initial conditions at the first thermal pulse till the 60th pulse. The dashed line corresponds to the underlying $M_{\rm c}-L$ relation adopted in this case, which is given by Eq. (6) multiplied by a factor of 1.16. The evolution of a 2.5 $M_\odot$ star with no envelope burning is also plotted. See the text for more details.
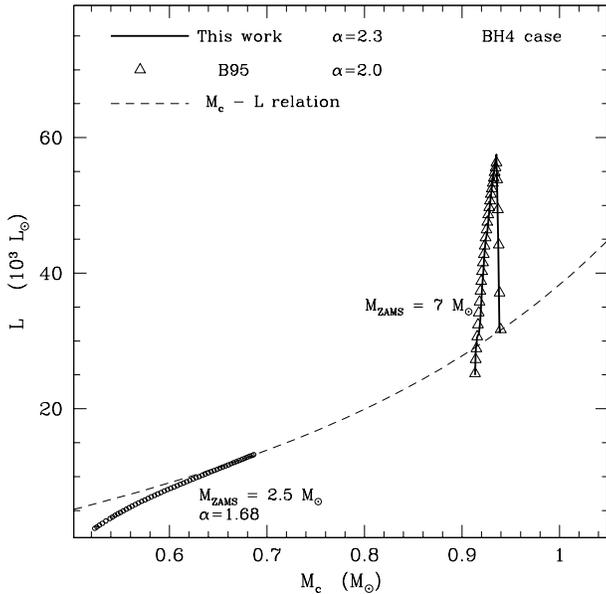
Fig. 2. The same as in Fig. 2, but with a different prescription for mass-loss (*BH4 case*). The Baud & Habing's formula (1983), applied since the beginning of the AGB, is then replaced with a constant rate, $\dot{M} = 4 \times 10^{-4} \, M_\odot \, \mathrm{yr}^{-1}$, as soon the core mass has grown up to $0.93537 \, M_\odot$. The results of complete calculations are taken from Blöcker (1995).
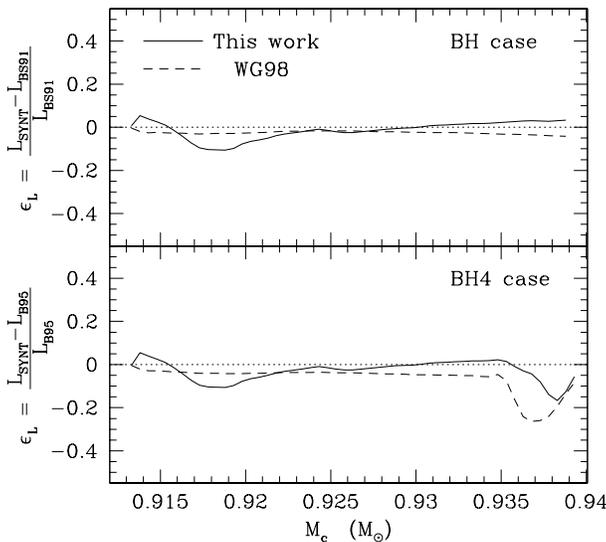
Fig. 3. Percentage difference in the estimation of the quiescent surface luminosity according to synthetic AGB calculations (L_{SYNT}) (by envelope integrations in this work (M98, solid line), and with the analytical fit of Eq. (5) by WG98 (dashed line), with respect to the results from complete calculations (L_{BS91} and L_{B95}), as a function of the core mass for an evolving $7 \, M_\odot$ star. Top and bottom panels refer to the *BH case* and *BH4 case* for mass loss, respectively.

to the first thermal pulses, the behaviour of which is usually irregular and model dependent, and then hardly reproducible. In the BH4 case ϵ_L is mostly confined to few percents as well. An increasing trend (to modest values still) shows up in the very late few interpulse periods, which are characterised by the
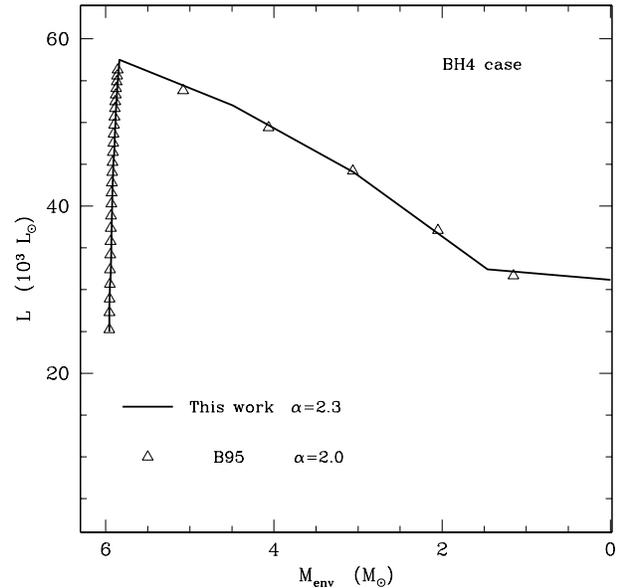
Fig. 4. Evolution of the surface luminosity for the $7 \, M_\odot$ AGB model as a function of the envelope mass, M_{env}, corresponding to *BH4 case* for mass loss. The notation is the same as in Fig. 1. Note the quick decline of the surface luminosity after the onset of the superwind.

drastic reduction of the envelope mass. The reason of this may be ascribed to somewhat different core mass-interpulse period relations (in Wagenhuber's (1996) and BS91 models). Then, given the extremely high mass-loss rate in these stages – when envelope burning is powering down but still operating – even a small a difference in the core mass just prior the occurrence of a thermal pulse can correspond to rather different values of the envelope mass, and hence of the expected surface luminosity.

A similar check is performed using the analytical fit suggested by WG98 and quoted in Eq. (5). The term (5c), expressing the luminosity contribution from envelope burning, is evaluated by setting $\alpha = 2.0$, as employed by BS91. The agreement with full calculations also turns out to be really good in both cases as illustrated in Fig. 3.

However, the advantage of our method, based on envelope integrations during the evolutionary calculations, is that it not only gives an estimate of L_{EB} and hence of the actual stellar luminosity (as the analytical fit by WG98 does), but the entire envelope structure of the star is consistently determined at each time step. This aspect is relevant, for instance, to the analysis of the nucleosynthesis due to envelope burning, which is followed in detail by integrating the nuclear network, once the density and temperature stratifications across the envelope are known. Moreover, the envelope model allows to check the sensitivity of the results to possible changes of the input physics (e.g. opacities, nuclear rates, mixing scheme).

Finally, Fig. 4 shows the surface luminosity of the $7 \, M_\odot$ star as a function of the envelope mass, with reference to the *BH4 case* for mass loss (in analogy with Fig. 9 in B95). The agreement of synthetic results (solid line) with complete calculations (empty triangles) is again very good, indicating that the method

is reliable to estimate the current strength of envelope burning as the envelope mass is being reduced by stellar winds.

4. Synthetic evolutionary calculations

The present paper is the first of a series devoted to present the results coming out from an extensive synthetic analysis of the TP-AGB evolution.

Evolutionary calculations have been carried out to follow the TP-AGB phase (from the first thermal pulse until the ejection of the envelope) for a dense grid stellar models with initial masses in the range $0.8 \, M_\odot \div 5 \, M_\odot$, and three values of the original chemical composition, $[X = 0.708, Y = 0.273, Z = 0.019]$, $[X = 0.742, Y = 0.250, Z = 0.008]$, and $[X = 0.756, Y = 0.240, Z = 0.004]$ (Marigo 1998, PhD Thesis). For each stellar model the initial conditions at the first thermal pulse are extracted from full calculations performed by means of the Padua stellar evolution code (Girardi & Bertelli 1998; Girardi et al. 1998, in preparation).

We remind the reader that the inclusion of moderate overshoot from core and external convection (Chiosi et al. 1992; Alongi et al. 1993) leads to a lower value of the maximum mass ($M_{\rm up} \sim 5 \, M_\odot$) for a star to pass through the AGB phase, than predicted by classical models without overshooting ($M_{\rm up} \sim 7$-$8 \, M_\odot$). For the evolutionary phases prior to the TP-AGB, the extension of the overshoot regions is governed by the parameters $\Lambda_{\rm c}$ and $\Lambda_{\rm e}$ relating the mean free path of the convective elements to the local pressure scale height, H_P, for core and envelope overshoot, respectively. Specifically, $\Lambda_{\rm c}$ is assumed to vary within the mass range ($\Lambda_{\rm c} = 0$ for $M/M_\odot \leq 1$; $\Lambda_{\rm c} = M/M_\odot - 1.0$ for $1.0 < M/M_\odot \leq 1.5$; $\Lambda_{\rm c} = 0.5$ for $M/M_\odot > 1.5$), whereas $\Lambda_{\rm e} = 0.25$ is adopted for all masses. For the sake of simplicity, no overshoot is applied to envelope integrations carried in synthetic TP-AGB calculations. The inclusion of convective overshoot to the envelope would determine higher temperatures at its base, thus strengthening the efficiency of envelope burning. Since a similar effect is produced by increasing the mixing-length parameter α, we presently prefer analysing the sensitiveness of the results to α rather than introducing an additional parameter (i.e. $\Lambda_{\rm e}$).

The analytical ingredients of the TP-AGB model are the same ones as in Marigo et al. (1996a, 1998), with some updates already presented in Sects. 2.1 and 2.2. We recall that the adopted prescription for mass loss is that by Vassiliadis & Wood (1993). The basic physical inputs employed in the static envelope model are the following. Nuclear reaction rates are those compiled by Caughlan & Fowler (1988), the screening factors are given by Graboske et al. (1973). At high temperatures ($T > 10^4$ K) stellar opacities are taken from Iglesias & Rogers (1996) (OPAL), at low temperatures ($T < 10^4$ K) the opacity tables by Alexander & Ferguson (1994) are used. The value $\alpha = 1.68$ adopted in envelope integrations derives from the calibration of the solar model (Girardi et al. 1996), which we usually refer to as the *standard case*. For purpose of comparison, other values are also used in the computation of envelope models (i.e. $\alpha = 2.0$ and $\alpha = 2.5$).

4.1. An improved treatment of the third dredge-up

The usual treatment of the third dredge-up in synthetic calculations is based on the adoption of two free parameters, namely: the efficiency λ, and the minimum core mass for convective dredge-up $M_{\rm c}^{\rm min}$. They are calibrated so as to fit some basic observational constraint, e.g. the observed luminosity function of carbon stars in the LMC ($M_{\rm c}^{\rm min} = 0.58 \, M_\odot$ and $\lambda \sim 0.6 - 0.7$ according to Groenewegen & de Jong (1993) and Marigo et al. (1996a)). The main purpose is to provide useful indications on the real occurrence of convective dredge-up, given the large degree of uncertainty still affecting the present understanding of this process in complete analyses of thermal pulses.

However, a weak point of synthetic models is the assumption that both dredge-up parameters are constant, regardless of the stellar mass and metallicity. On the contrary, complete models of AGB stars indicate that the onset of dredge-up (related to $M_{\rm c}^{\rm min}$) and its efficiency (related to λ) is favoured in stars of higher masses and lower metallicities (Wood 1981; Boothroyd & Sackmann 1988b).

In this work, this limitation of synthetic models is partially overcome. In Marigo et al. (1998, in preparation) an exhaustive description of the method is presented. Suffice it to formulate here the basic concepts.

According to the results from detailed calculations of thermal pulses it turns out that, at the stage of the post-flash luminosity peak, the penetration of envelope convection into the intershell region would occur only if the base temperature, $T_{\rm b}$, approaches or exceeds some critical value $T_{\rm b}^{\rm dred}$, which turns out to be almost independent from $M_{\rm c}$ and Z (e.g. $\log T_{\rm b}^{\rm dred} \sim 6.7$ as indicated by Wood (1981); $\log T_{\rm b}^{\rm dred} \sim 6.5$ according to Boothroyd & Sackmann 1988b). As already pointed out by Wood (1981), this useful indication provides the basic criterion to infer *if and when* dredge-up takes place. The use of $M_{\rm c}^{\rm min}$ is then abandoned. Of course, the critical value for $T_{\rm b}^{\rm dred}$ is a free parameter as well, which must be calibrated on the basis of some observational constraint.

However, the improvement is real. Every time a thermal pulse is expected during calculations, envelope integrations are performed to check whether the condition on the base temperature is satisfied. It follows that, contrary to the test based on the constant $M_{\rm c}^{\rm min}$ parameter, with this scheme the response depends not only on the core mass but also on the current physical conditions of the envelope (i.e. the surface luminosity peak, the effective temperature, the mass, the chemical composition). Moreover, this method allows to determine not only the onset, but also the possible shut-down of dredge-up occurring when the envelope mass is significantly reduced by stellar winds.

We are aware of the fact that such treatment of the third dredge-up is still an approximation of the real process, mostly because the efficiency λ is not expected to be constant, but to vary with envelope mass, pulse strength, mixing-length parameter, treatment of convection (see, for instance, Frost & Lattanzio 1996; Wood 1997; Herwig et al. 1997). However, we believe that this approach is what can be presently done best in synthetic TP-AGB models, given the impossibility to derive

a well-established quantitative prescription for λ from detailed analyses of thermal pulses. In this perspective, more complete calculations of the third dredge-up, consistent with observations, are needed.

As already mentioned, the dredge-up parameters, λ and $T_{\rm b}^{\rm dred}$, need to be specified. The carbon star luminosity functions (CSLFs) in the LMC and SMC provide the observational constraint. According to Marigo (1998, Phd Thesis), the calibration for the LMC yields $\lambda = 0.50$ and $T_{\rm b}^{\rm dred} = 6.4$, whereas for the SMC we get $\lambda = 0.65$ and $T_{\rm b}^{\rm dred} = 6.4$. Then, a higher efficiency of convective dredge-up seems to be required at lower metallicities, which would agree with predictions by full calculations.

In this way we fix the values of the dredge-up parameters adopted during the present calculations for different metallicity sets. Specifically, the calibration based on the CSLF in the LMC is applied to TP-AGB models with metallicities $Z = 0.008$, the reproduction of the CSLF in the SMC specifies the dredge-up parameters for TP-AGB models with $Z = 0.004$. The former calibration is applied also to the metallicity set $Z = 0.019$, even if a lower λ would be suggested by extrapolating from the $Z = 0.008$ and $Z = 0.004$ cases.

Regarding the stellar models studied in this work (with $3.5\,M_\odot \leq M \leq 5.0\,M_\odot$), it turns out that envelope burning, as expected, prevents the conversion to carbon stars for most of their TP-AGB phase because of the efficient nuclear transmutation of newly dredged-up carbon into nitrogen. Possible transitions to the C-class may occur either early in the evolution when dredge-up still dominates over weak (but growing in efficiency) envelope burning, or in the very late stages as envelope burning extinguishes and a few more dredge-up events possibly take place. All these aspects are analysed and discussed in Marigo et al. (1998, in preparation).

4.2. Evolution in the $M_{\rm c} - L$ diagram

Fig. 5 shows the luminosity evolution described by TP-AGB stars with initial metallicity $Z = 0.008$ as a function of core mass, according to the *standard case* (i.e. $\alpha = 1.68$). Each symbol along the curves refers to the quiescent pre-flash luminosity maximum, just before the occurrence of a thermal pulse. The dot-dashed line corresponds to the standard $M_{\rm c} - L$ relation valid for full amplitude regime with no envelope burning. It is expressed by Eq. (6) with the term (6c) set equal to zero, as this refers to the first pulses which are not yet in the asymptotic regime. Three points are worthy to be remarked.

First, all the tracks are characterised by an initial subluminous evolution typical of the first thermal pulses, below the $M_{\rm c} - L$ relation. The apparent late merging of these models to the $M_{\rm c} - L$ relation is due to the early onset of the third dredge-up, as already pointed out when discussing (see Sect. 3) the luminosity evolution of the $2.5\,M_\odot$ star shown in Figs. 1 and 2.

Second, as soon as the standard relation is approached, stars with mass $M \lesssim 3.5\,M_\odot$ increase their luminosity closely following the same relation till the end of evolution, regardless of
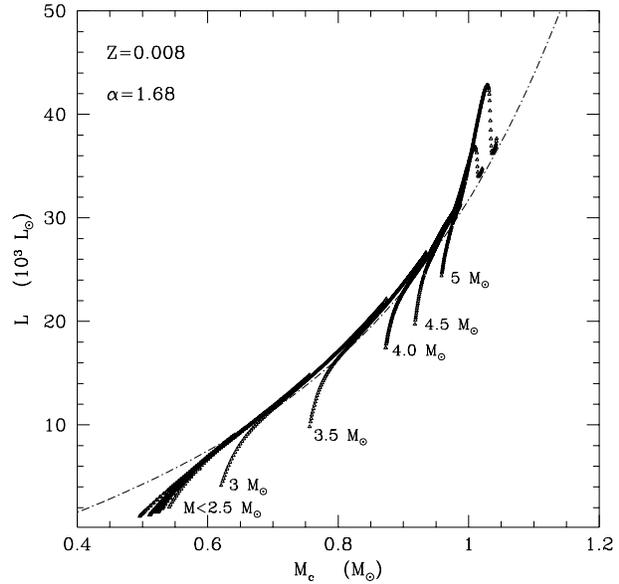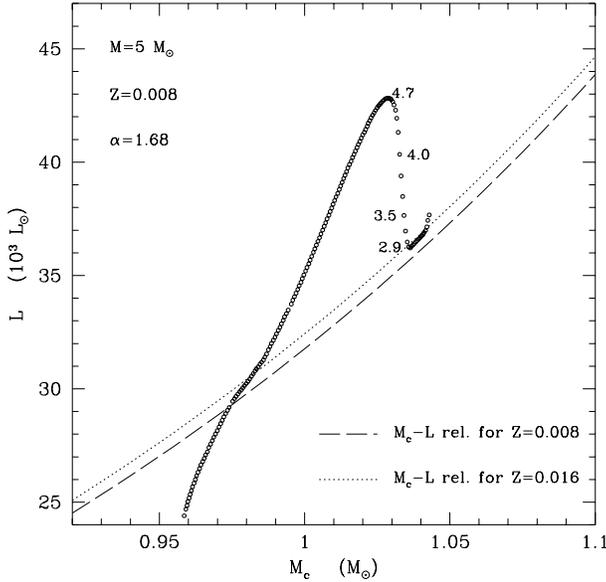

Fig. 5. Quiescent luminosity evolution as a function of the core mass for TP-AGB stars with initial chemical composition $[X = 0.742, Y = 0.250, Z = 0.008]$, and mass as indicated nearby the corresponding track. Symbols correspond to the pre-flash luminosity maximum before the occurrence of each thermal pulse. The dot-dashed line represents the $M_{\rm c} - L$ relation for $Z = 0.008$.

the current value of the envelope mass. Quite a different behaviour characterises the luminosity evolution of more massive stars ($3.5\,M_\odot < M \leq 5\,M_\odot$), departing from the $M_{\rm c} - L$ relation because of the occurrence of envelope burning. This aspect will be discussed in detail in Sect. 5.

Third, we can notice that in the cases with no envelope burning, stars may not exactly obey the relation shown in Fig. 5, but evolve towards slightly higher luminosities, in particular during the last evolutionary stages.

This can be explained considering that the plotted $M_{\rm c} - L$ relation refers to a given value of the metallicity, $Z = 0.008$, so that the weighting factor, $3980 \log(Z/0.02)$, in the term (6a) is constant. However, during calculations we take into account the possible increase of the effective metallicity, defined as $Z = 1 - X - Y$, due to the surface chemical enrichment produced by convective dredge-up, and possibly by envelope burning. Therefore, for a given core mass the luminosity is expected to be higher at increasing metallicity. The effect is more pronounced after the last dredge-up episodes, when the dilution of newly synthesised elements involves a smaller residual envelope mass. To this respect, an example is illustrated in Fig. 6, referring to the $(5\,M_\odot, Z = 0.008)$ TP-AGB model experiencing both dredge-up events and envelope burning (see also Sect. 5.1). The effective metallicity has increased up to $Z = 0.0126$ at the stage of the peak luminosity (with a current mass of about $4.7\,M_\odot$), and to $Z = 0.0132$ at the recovering of the $M_{\rm c} - L$ relation (when the mass is reduced down to $2.9\,M_\odot$). The last dredge-up episodes produce a further increment of the metallicity which attains a maximum value of $Z = 0.0258$ at the end of TP-AGB calculations. Similar results hold for the other two sets of TP-

Fig. 6. Quiescent luminosity evolution of a $5.0\,M_\odot$, $Z = 0.008$ star experiencing envelope burning. The open circles correspond to the maximum quiescent luminosity before each He-shell flash. The numbers along the curve indicate the current stellar mass in solar units. The dashed and dotted lines represent the reference $M_c - L$ relation for $Z = 0.008$ and $Z = 0.016$, respectively.

AGB models here considered (with metallicities $Z = 0.019$ and $Z = 0.004$).

5. Over-luminosity produced by envelope burning

As already mentioned, the energy contribution from envelope burning makes massive TP-AGB stars leave the $M_c - L$ relation during part of their evolution. In this study we analyse the dependence of envelope burning on three basic parameters namely, the mass of the star M, the metallicity Z of the envelope, and the mixing-length parameter, $\alpha = \Lambda/H_P$, where Λ is the mixing length according to the classical theory of convection (Mixing Length Theory; Böhm-Vitense 1958), and H_P is the pressure scale-height. The results are clearly illustrated in Figs. 7–9, referring to TP-AGB stars with initial mass of 3.5, 4.0, 4.5, and $5.0\,M_\odot$ for three values of the initial metallicity, $Z = 0.019$, $Z = 0.008$, and $Z = 0.004$, respectively. For each star of given mass and chemical composition, envelope integrations are carried out adopting three values of the mixing-length parameter, $\alpha = 1.68$ (*standard case*), $\alpha = 2.00$, and $\alpha = 2.50$.

We can notice that for particular combinations of the stellar parameters here considered (i.e. lower M, higher Z, and lower α, as in the ($3.5\,M_\odot$, $Z = 0.019$, $\alpha = 1.68$) model of Fig. 7), envelope burning does not develop or it is so weak that the over-luminosity effect does not show up and the the evolution of the quiescent luminosity complies with the $M_c - L$ relation. Actually, it turns out that the limiting stellar mass for the development of envelope burning heavily depends on Z and α. For instance, the *standard case* with $Z = 0.019$ and $\alpha = 1.68$ shows en-

velope burning for $M \gtrsim 4.5\,M_\odot$, and only a high value of α (i.e. 2.5) drops this transition mass down to $3.5\,M_\odot$ (see also Table 2).

We specify that the results for the ($5.0\,M_\odot$, $Z = 0.004$) model are not actually present since this is just a limit case. The stellar mass slightly exceeds the critical value M_{up} for that metallicity, so that carbon ignition has occurred before the onset of the thermally pulsing regime.

It is worth remarking that M, Z, and α significantly affect the luminosity evolution of a star with envelope burning as long as the stellar mass is not so dramatically lowered, before the re-approaching onto the $M_c - L$ relation. This corresponds to most of the TP-AGB duration, since high mass-loss rates are typically attained at the very end of the evolution (Vassiliadis & Wood 1993). Once the super-wind regime has developed, the subsequent luminosity evolution is crucially controlled by the efficiency of mass loss in reducing the envelope mass down to the complete ejection. An earlier onset of the super-wind would favour an earlier extinction of envelope burning and, correspondingly, a lower maximum luminosity would be reached by the star before the subsequent decline towards the $M_c - L$ relation. In principle, the onset of the super-wind regime as soon as the star enters the AGB phase may even prevent the occurrence of envelope burning.

In the following discussion we will consider the effects produced by varying M, Z, and α, for a given mass-loss prescription (i.e. Vassiliadis & Wood 1993). The main results relevant to the present analysis are indicated in Table 2.

5.1. The dependence on M

For fixed Z and α, envelope burning is expected to be more efficient in stars of greater mass. From Figs. 7–9 it turns out that the maximum excursion of the luminosity above the $M_c - L$ relation is higher in initially more massive models (see also the M_{bol}^{peak} enter in Table 2). Moreover, the development of envelope burning crucially depends on the current envelope mass during the evolution. This effect is exemplified in Fig. 6, referring to the case of the ($5\,M_\odot$, $Z = 0.008$, $\alpha = 1.68$) model. This behaviour of the luminosity agrees with the results from full evolutionary calculations of the TP-AGB phase (e.g. B95; Boothroyd & Sackmann 1992; Vassiliadis & Wood 1993).

Envelope burning develops since the first sub-luminous interpulse periods, so that when thermal pulses attain the full-amplitude regime the star does not settle on the $M_c - L$ relation (dashed line), but quickly reaches higher and higher luminosities, with a brightening rate (few times $-10^{-6} \div -10^{-5}$ mag yr^{-1}; see the $\dot{M}_{bol}$ entry in Table 2), much greater than expected from the slope of the standard relation (typically $-7 \div -9 \times 10^{-7}$ mag yr^{-1}).

The luminosity growth goes on as long as the envelope remains massive enough to support high envelope base temperatures ($T_b > 40 - 60 \times 10^6\,K$). In fact, the luminosity decline after the maximum is concomitant with the onset of the super-wind, when the star starts to rapidly lose mass at significant rates (i.e. $\dot{M} \sim 10^{-5} \div 10^{-4}\,M_\odot$ yr^{-1}). This drastically weak-
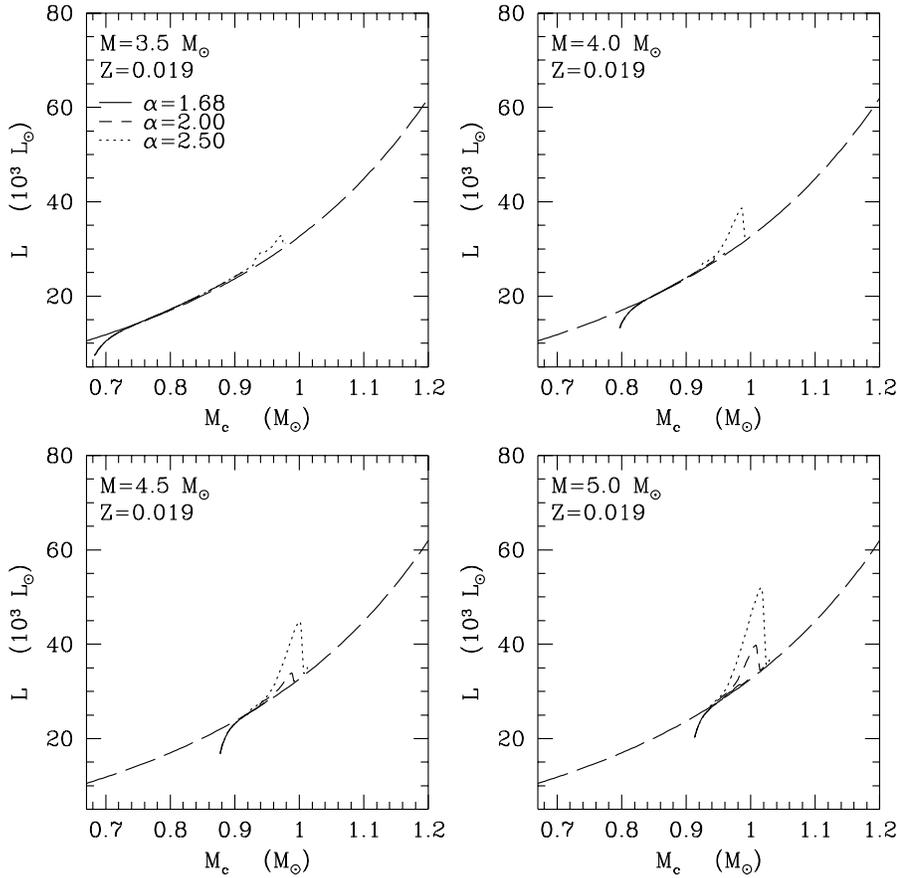
Fig. 7. Luminosity evolution of 3.5, 4.0, 4.5, 5.0 $M_\odot$ TP-AGB model stars with initial metallicity $Z = 0.019$ as a function of the core mass for three values of the mixing-length parameter, α, as indicated. Stellar luminosities refer to the pre-flash maximum stage. The long-dashed lines correspond to the reference standard core mass-luminosity relation.

ens the efficiency of envelope burning so that, finally, the over-luminosity vanishes and the star approaches again the $M_c - L$ relation where it remains during the very last stages till the end of evolution. To this respect, we can notice that the final re-covering of the $M_c - L$ relation (dotted line) is consistent with an effective metallicity ($Z = 0.016$) that is twice the value at the beginning of the TP-AGB phase ($Z = 0.008$; dashed line), because of the occurrence of both dredge-up and envelope burning.

In Table 2 we also indicate the value of the envelope mass at the shut-down of envelope burning ($M_{env}(noEB)$ entry), i.e. when its contribution to the stellar luminosity has decreased to less than 1%. Note that $M_{env}(noEB)$ is not constant at all, but it varies mostly in the range between roughly $2\,M_\odot$ and $0.5\,M_\odot$. It results that the more efficient envelope burning has been (e.g. for larger M, lower Z, higher α), the smaller is this critical value of the envelope mass.

5.2. The dependence on Z

At given M and α, the over-luminosity is more pronounced at lower metallicities. It is worth remarking that the direct effect of chemical composition on the base temperature is negligible itself (Sackmann & Boothroyd 1991). The greater efficiency of envelope burning is mostly due to the fact that a star of given M enters the AGB phase with a core mass, M_c, that is greater for decreasing metallicity (see for example the $M_{c,0}$ entry in

Table 2). Considering that in the deepest layers of the envelope close to the core, the radiative gradient depends like $\nabla_r \propto M_c^\gamma$, where γ is always positive ($0.5 \div 2.5$, as indicated by Scalo et al. 1975), it follows that a deeper penetration of external convection is expected for higher values of the core mass, and hence for lower metallicities.

5.3. The dependence on α

The dependence of envelope burning on α is remarkable as already pointed out by various authors (Sackmann & Boothroyd 1991; D'Antona & Mazzitelli 1996). An increase of α causes an overall local rise of the temperature profile across the envelope, so that both the effective temperature, T_{eff}, and the base temperature, T_b, are hotter. It follows that α affects both the external configuration of an AGB star (i.e. the position on the H-R diagram), and its internal structure (i.e. the temperature stratification of the convective envelope and related nuclear energy generation). In particular, the higher temperatures, attained at the base of the convective envelope at increasing α, determine a stronger efficiency of nuclear burning. This is evident in Figs. 7–9 from the greater amplitude of the luminosity excursion in models with the same mass and metallicity (see also the M_{bol}^{tip} and $(L_{EB}/L)_{max}$ entries in Table 2).

However, changing the value of the mixing-length parameter produces important consequences which are not merely re-
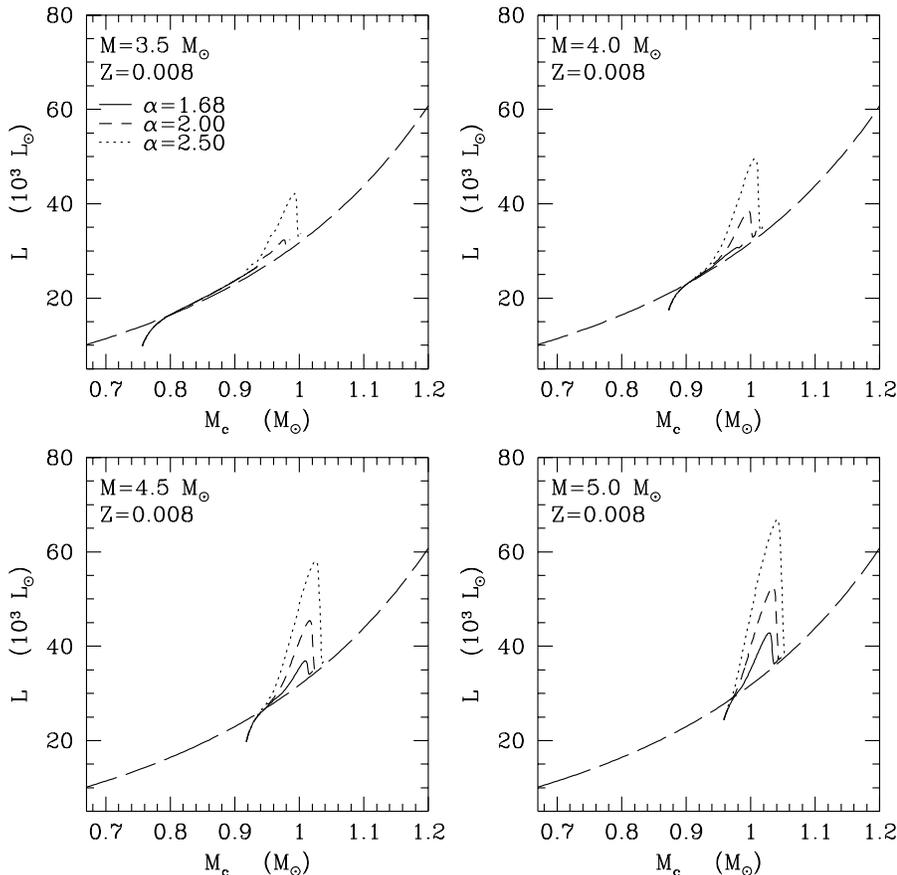
Fig. 8. The same as in Fig. 7, but with $Z = 0.008$.
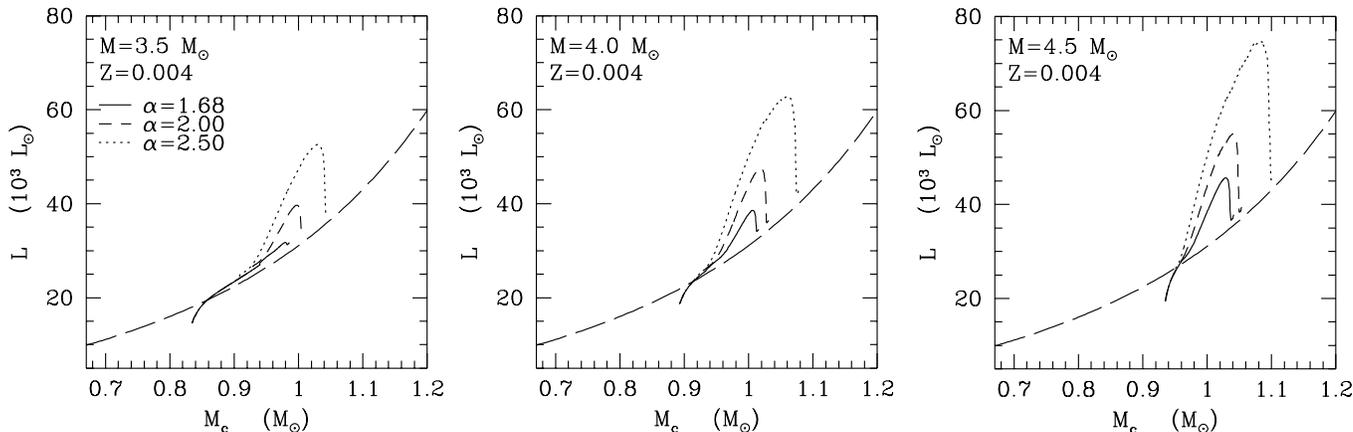
Fig. 9. The same as in Fig. 7, but with $Z = 0.004$.

lated to the efficiency of envelope burning, but deal with further aspects of the evolution of these stars.

A notable point concerns mass loss, and consequently the TP-AGB lifetimes (see the $\tau_{\mathrm{TP-AGB}}$ entry in Table 2). From our analysis it turns out that for a given model, the onset of the super-wind regime is delayed for higher values of the mixing-length parameter. Consequently, for given initial mass and metallicity the whole duration of the TP-AGB phase is longer for a star with a more efficient envelope burning obtained by increasing α. This result does not contradict the result that the high luminosities produced by envelope burning would anticipate the end the evo-

lution by triggering enhanced mass-loss rates (see for example BS91). To clarify this point, let us consider the competition between luminosity and effective temperature in determining the efficiency of mass loss. According to Vassiliadis & Wood's prescription (1993), adopted in our calculations, the dependence of the mass-loss rate before the development of the superwind, can be expressed as $\log \dot{M} \propto P \propto T_{\mathrm{eff}}^{-3.88} L^{0.97} M^{-0.9}$, where P is the fundamental period of pulsation. Hence, an increase of α operates in two opposite directions. From one side, it favours mass loss via the term $L^{0.97}$, as it strengthens the efficiency of envelope burning, quickly leading to higher luminosities. From

Table 2. Properties of TP-AGB stars with envelope burning.

Z	α	$M_{\rm i}$	$M_{\rm c,0}$	$\tau_{\rm TP-AGB}$	$M_{\rm f}$	$M_{\rm bol}^{\rm tip}$	$M_{\rm bol}^{\rm peak}$	$(L_{\rm EB}/L)_{\rm max}$	$M_{\rm env}({\rm no\,EB})$
0.019	1.68	3.5	0.683	1.623E+06	0.845	−6.035	...............No over-luminosity...............		
		4.0	0.797	7.372E+05	0.896	−6.211	...............No over-luminosity...............		
		4.5	0.877	4.312E+05	0.951	−6.402	...............No over-luminosity...............		
		5.0	0.913	4.139E+05	0.996	−6.558	−6.525	0.010	2.991
	2.00	3.5	0.683	2.056E+06	0.912	−6.281	...............No over-luminosity...............		
		4.0	0.797	1.099E+06	0.960	−6.441	−6.428	0.016	2.264
		4.5	0.877	6.593E+05	0.998	−6.568	−6.604	0.065	1.978
		5.0	0.913	5.129E+05	1.020	−6.644	−6.779	0.154	1.879
	2.50	3.5	0.683	2.391E+06	0.979	−6.518	−6.570	0.067	1.465
		4.0	0.797	1.253E+06	0.994	−6.564	−6.747	0.178	1.202
		4.5	0.877	7.205E+05	1.013	−6.645	−6.909	0.265	1.119
		5.0	0.913	5.427E+05	1.029	−6.695	−7.069	0.334	1.146
0.008	1.68	3.5	0.756	1.451E+06	0.935	−6.345	...............No over-luminosity...............		
		4.0	0.873	6.990E+05	0.987	−6.521	−6.500	0.011	2.239
		4.5	0.918	5.327E+05	1.021	−6.632	−6.697	0.097	1.891
		5.0	0.958	3.853E+05	1.043	−6.720	−6.859	0.175	1.905
	2.00	3.5	0.756	1.711E+06	0.985	−6.556	−6.554	0.053	1.599
		4.0	0.873	7.935E+05	1.008	−6.618	−6.745	0.164	1.268
		4.5	0.918	5.645E+05	1.027	−6.655	−6.923	0.250	1.247
		5.0	0.958	3.990E+05	1.047	−6.721	−7.083	0.316	1.234
	2.50	3.5	0.756	1.779E+06	1.002	−6.601	−6.843	0.234	0.880
		4.0	0.873	8.279E+05	1.019	−6.662	−7.018	0.328	0.751
		4.5	0.918	6.025E+05	1.039	−6.720	−7.188	0.393	0.776
		5.0	0.958	4.018E+05	1.054	−6.745	−7.343	0.450	0.662
0.004	1.68	3.5	0.834	1.409E+06	0.986	−6.535	−6.534	0.025	1.721
		4.0	0.893	9.694E+05	1.016	−6.627	−6.746	0.134	1.586
		4.5	0.935	7.378E+05	1.041	−6.725	−6.929	0.220	1.447
	2.00	3.5	0.834	1.517E+06	1.007	−6.613	−6.777	0.171	1.021
		4.0	0.893	1.041E+06	1.031	−6.694	−6.970	0.270	1.109
		4.5	0.935	7.736E+05	1.054	−6.769	−7.131	0.327	1.045
	2.50	3.5	0.834	1.660E+06	1.045	−6.749	−7.082	0.305	0.639
		4.0	0.893	1.165E+06	1.078	−6.862	−7.276	0.361	0.714
		4.5	0.935	8.882E+05	1.102	−6.940	−7.463	0.427	0.551

- Z: initial metallicity
- $M_{\rm i}$: initial mass at the ZAMS ($M_\odot$)
- $M_{\rm c,0}$: core mass at the onset of the TP-AGB phase ($M_\odot$)
- $\tau_{\rm TP-AGB}$: TP-AGB lifetime (yr)
- $M_{\rm f}$: final mass ($M_\odot$)
- $M_{\rm bol}^{\rm tip}$: bolometric magnitude at the tip of the AGB
- $M_{\rm bol}^{\rm peak}$: bolometric magnitude at the maximum efficiency of envelope burning, before the onset of the super-wind phase
- $(L_{\rm EB}/L)_{\rm max}$: maximum relative contribution of envelope burning to the surface luminosity
- $M_{\rm env}({\rm no\,EB})$: envelope mass at the extinction of envelope burning ($M_\odot$)

the other side, it weakens mass loss via the term $T_{\rm eff}^{-3.88}$, as it reduces the stellar radius, yielding higher values of the effective temperature. The net result depends on the prevailing effect, that in our case turns out to be related to the increase of the effective temperature. It is interesting to notice, however, that different formulations for mass loss could produce different results, owing to their specific dependence on stellar parameters, i.e. luminosity and effective temperature.

6. Concluding remarks

In this study it has been shown that the break-down of the $M_{\rm c}-L$ relation and the related over-luminosity effect produced by the occurrence of envelope burning in the most massive TP-AGB stars can be consistently taken into account in synthetic calculations. In fact, the original method based on envelope integrations is able to successfully reproduce the results of complete evolutionary models.

This nice result strengthens the reliability of envelope integrations in synthetic TP-AGB models for various related aspects, such as the nucleosynthesis occurring in hot bottom envelopes and the chemical yields.

The results of the present paper derive from extensive calculations of the AGB phase carried out for a fine grid of stellar masses ($0.8\,M_\odot \lesssim M \leq 5\,M_\odot$) and various metallicities ($Z = 0.019$, $Z = 0.008$, and $Z = 0.004$). This work is actually a part of a project aimed at investigating various aspects of the AGB evolution by means of a flexible and accurate synthetic model. If the flexibility is an intrinsic characteristic of synthetic codes, this model gains in accuracy thanks to the use of analytical prescriptions derived from detailed AGB calculations (e.g. Wagenhuber 1996), coupled to a complete envelope model updated with recent input physics (i.e. opacities, nuclear reactions rates).

Up-coming papers are devoted to present and analyse other issues of interest. In particular, basing on the improved treatment of the third dredge-up included in synthetic calculations (briefly outlined in Sect. 4.1) we will address the question of reproducing the luminosity functions of carbon stars in both the LMC and SMC (Marigo et al. 1998, in preparation). A further work will be dedicated to present the results on the predicted changes in the surface chemical abundances of AGB stars and related chemical yields, as a function of the stellar mass and metallicity (Marigo et al. 1998, in preparation).

References

Alexander D.R., Ferguson J.W., 1994, ApJ 437, 879
Alongi M., Bertelli G., Bressan A., et al., 1993, A&AS 97, 851
Baud B., Habing H.J., 1983, A&A 127, 73
Blöcker T., 1995, A&A 297, 727 (B95)
Blöcker T., Schönberner D., 1991, A&A 244, L43 (BS91)

Böhm-Vitense E., 1958, Z. Astrophys. 46, 108
Boothroyd A.I., Sackmann I.-J., 1988a, ApJ 328, 641
Boothroyd A.I., Sackmann I.-J., 1988b, ApJ 328, 671
Boothroyd A.I., Sackmann I.-J., 1992, ApJ 393, L21
Bragaglia A., Renzini A., Bergeron P., 1995, ApJ 443, 735
Caughlan G.R., Fowler W.A., 1988, Atomic Data Nucl. Data Tables 40, 283
Chiosi C., Bertelli G., Bressan A., 1992, ARA&A 30, 305
Cox A.N., Stewart J.N., 1970, ApJS 19, 243
D'Antona F., Mazzitelli I., 1996, ApJ 470, 1093
Frost C.A., Lattanzio J.C., 1996, ApJ 473, 383
Girardi L., Bertelli G., 1998, MNRAS, in press
Girardi L., Bressan A., Chiosi C., Bertelli G., Nasi E., 1996, A&AS 117, 113
Graboske H.C., de Witt H.E., Grossman A.S., Cooper M.S., 1973, AJ 181, 457
Groenewegen M.A.T., de Jong T., 1993, A&A 267, 410
Herwig F., Blöcker T., Schönberner D., El Eid M., 1997, A&A L324
Iben I., Renzini A., 1983, ARA&A 21, 27
Iben I., Truran J.W., 1978, ApJ 220, 980
Iglesias C.A., Rogers F.J., 1996, ApJ 464, 943
Kippenhahn R., Weigert A., Hofmeister E., 1967, In: Alder B., Fernbach S., Rotenberg M. (eds.) Methods in Computational Physics, New York: Academic Press Vol. 7, p. 129
Lattanzio J.C., 1992, Proc. Astron. Soc. Austr. 10, 120
Marigo P., Bressan A., Chiosi C., 1996a, A&A 313, 545
Marigo P., Girardi L., Chiosi C., 1996b, A&A 316, L1
Marigo P., Bressan A., Chiosi C., 1998, A&A 331, 564
Marigo P., 1998, PhD thesis, University of Padova
Paczyński B., 1970, Acta Astron. 20, 47
Renzini A., Voli M., 1981, A&A 94, 175
Sackmann I.-J., Boothroyd A.I., 1991, ApJ 366, 529
Scalo J.M., Despain K.H., Ulrich R.K., 1975, ApJ 196, 805
Vassiliadis E., Wood P.R, 1993, ApJ 413, 641
Wagenhuber J., 1996, PhD thesis, TU München
Wagenhuber J., Groenewegen M.A.T., 1998, A&A, accepted (WG98)
Wood P.R., 1981, in: Physical processes in red giants, Proc. of the Second Workshop, Erice, Italy, (September 3-13, 1980), Dordrecht, D. Reidel Publishing Co., p. 135-139
Wood P.R., 1997, In: Habing H.J., Lamers H.J.G.L.M. (eds.) Planetary Nebulae, Proc. of IAU Symposium No. 180, Groeningen, The Netherlands, (August 26-30, 1996), Kluwer Academic Publishers, p. 297-302
Wood P.R., Bessell M.S., Fox M.W., 1983, ApJ 272, 99